Journal of Plant Physiology 325 (2026) 154850

Contents lists available at ScienceDirect

Journal of Plant Physiology

journal homepage: www.elsevier.com/locate/jplph

N_2-induced hypoxia and waterlogging elicit distinct whole-plant transpiration and adventitious-root responses in tomato (*Solanum lycopersicum*)

Hermann Prodjinoto [a], Dor Batat [a], Ido Nir [c], Dana Menkes [b], Moshe Shenker [b], Menachem Moshelion [a,*]

[a] Institute of Plant Sciences and Genetics in Agriculture, The Robert H. Smith Faculty of Agriculture, Food and Environment, The Hebrew University of Jerusalem, Rehovot, 76100, Israel
[b] Department of Soil and Water Sciences, Institute of Environmental Sciences, Faculty of Agriculture, Food and Environment, The Hebrew University of Jerusalem, Rehovot, 76100, Israel
[c] The Institute of Plant Sciences, Agricultural Research Organization, The Volcani Center, 68 HaMaccabim Road, P.O.B. 15159, Rishon LeZion, 7505101, Israel

ARTICLE INFO

Keywords:
Tomato
Waterlogging
N_2-induced hypoxia
Transpiration dynamics
Adventitious roots
Rhizosphere redox
Gravimetric phenotyping
Root hydraulics

ABSTRACT

Waterlogging constrains terrestrial plants by limiting gas diffusion and altering the hydraulic and chemical environment of roots. Yet it remains unclear which whole-plant responses arise from oxygen limitation alone and which require the broader physical context of excess water. Using high-resolution gravimetric lysimetry in tomato, we compared N_2-induced hypoxia under near-field-capacity conditions with root-zone waterlogging. N_2 injection reduced root-zone O_2 from approximately 18%–19% to below 1% and altered pH, redox potential, and mineral relations, but whole-plant transpiration declined only after sustained exposure. Waterlogging caused a faster, genotype-dependent transpiration decline in M82, IL11-4, and IL8-1. Adventitious-root emergence at the soil–air interface coincided with transient partial recovery of transpiration, whereas stronger adventitious-root development occurred in plants with larger transpiration losses. The renewed decline in transpiration after drainage was consistent with a partial contribution of surface-associated adventitious roots, although restoration of drainage also altered root-zone aeration, water availability, and primary-root conditions and therefore did not isolate their specific contribution. Together, the distinct response kinetics and root phenotypes show that rapid N_2-induced hypoxia did not reproduce the full waterlogging response. Adventitious roots were induced most strongly under severe stress and were temporally associated with partial, but not complete, recovery of whole-plant transpiration.

1. Introduction

Plant transpiration drives the transport of water and minerals to photosynthetic tissues. Although soil water is required to sustain this process, excess water in the rhizosphere, through root-zone flooding or waterlogging, can disrupt water and mineral uptake and severely impair terrestrial plant performance. This threat is being amplified by climate change, which is increasing the frequency and intensity of heavy rainfall and flooding events. From 2000 to 2019, the global cropland area exposed to flooding increased by nearly 84,000 km^2, representing a 7.75% increase (Zhang et al., 2023). Currently, 24% of global cropland lies in flood-prone regions (Zhang et al., 2023), placing a substantial fraction of global crop-producing land at recurring risk. Waterlogging rapidly displaces air from soil pores and restricts gas exchange between the soil and the atmosphere, sharply reducing oxygen availability to roots (Colmer and Voesenek, 2009; Pezeshki and DeLaune, 2012). Oxygen deficiency, widely considered a primary cause of flooding injury in terrestrial plants, shifts root metabolism from aerobic respiration to anaerobic pathways and can create energy deficits that lead to progressive root damage (Colmer and Voesenek, 2009; Horchani et al., 2009; Pan et al., 2021). In tomato, flooded soils typically induce leaf wilting, epinasty, reduced shoot elongation, callus formation, adventitious-root emergence near the water surface, and chlorosis of older leaves (Jackson, 1956), while reducing transpiration and growth

* Corresponding author.
E-mail address: menachem.moshelion@mail.huji.ac.il (M. Moshelion).

https://doi.org/10.1016/j.jplph.2026.154850
Received 26 June 2026; Received in revised form 17 July 2026; Accepted 22 July 2026
Available online 27 July 2026

(Kuo and Chen, 1980). These observations raise a central question: which components of the waterlogging response can be reproduced by N_2-induced hypoxia under non-flooded conditions, and which responses are associated with the additional physical and hydraulic conditions created by excess water?

In addition to limiting oxygen supply, flooding alters rhizosphere chemistry. Low-oxygen conditions promote the accumulation of gases such as CO_2 and methane and stimulate anaerobic microbial processes, beginning with denitrification and, under more reducing conditions, progressing to the reduction of manganese, iron, and sulfate. These processes alter soil redox potential (Eh) and can strongly affect nutrient availability to plants (Colmer and Voesenek, 2009; Pezeshki and DeLaune, 2012). Consequently, nutrient uptake and transport may be impaired, potentially leading to deficiency or toxicity despite ongoing plant acclimation. For example, 2–7 days of flooding in barley reduced foliar N, P, and K concentrations by 50%–60%, illustrating how water excess can impair nutrient acquisition through both altered soil chemistry and oxygen-limited root function (Leyshon and Sheard, 1974). We therefore monitored rhizosphere pH and redox potential, characterized elemental composition in the soil solution and drainage, and quantified mineral composition in leaves and roots as part of testing whether oxygen depletion alone is sufficient to reproduce key waterlogging responses.

Under waterlogging, many terrestrial plants develop adventitious roots, typically emerging from the stem or lower shoot near the soil or water surface (Jackson, 1956; Sauter, 2013). These roots are commonly associated with flooded environments and have been widely linked to oxygen deficiency and ethylene signaling in the submerged root zone (McNamara and Mitchell, 1990; Vidoz et al., 2010; Kęska et al., 2021). However, adventitious-root formation is commonly observed under waterlogged conditions, where roots are exposed to free or near-surface water, suggesting that hypoxia may interact with the distinct hydraulic and physical configuration imposed by water excess. Unlike the primary root system embedded in soil, adventitious roots often develop at the soil–air or soil–water interface, where oxygen availability and water accessibility differ from those during N_2-induced hypoxia under non-flooded conditions. Although adventitious roots are often interpreted as an adaptive response that replaces or supplements the primary root system under flooding (Colmer and Voesenek, 2009; Calvo-Polanco et al., 2012; Sauter and Steffens, 2014; Zhang et al., 2017), their actual contribution to whole-plant water uptake and transpiration under tomato root-zone waterlogging remains incompletely quantified.

Despite extensive documentation of adventitious-root formation under flooding, two major gaps remain unresolved. First, many interpretations of flooding responses emphasize oxygen deficiency, whereas fewer studies experimentally compare hypoxia under non-flooded conditions with the physical conditions created by water excess, in which roots are exposed to free surface water rather than soil. It therefore remains unclear whether key physiological responses to flooding, including changes in transpiration and nutrient uptake, can be explained solely by oxygen limitation or instead reflect additional water-excess-specific constraints on whole-plant water relations. Second, although adventitious roots are widely interpreted as a functional replacement for the primary root system under flooded conditions, their hydraulic contribution at the whole-plant level has rarely been quantified. In particular, direct links among adventitious-root development, surface-associated water access, and whole-plant transpiration remain largely inferential in tomato root-zone waterlogging systems, limiting our ability to determine whether these roots are associated with partial maintenance of plant water balance, with flooding-stress severity, or with both processes.

The objective of this study was to test two related hypotheses using a two-step experimental framework. First, we imposed N_2-induced hypoxia under near-field-capacity, non-flooded conditions in tomato cv. M82, allowing us to test whether root-zone oxygen depletion alters whole-plant transpiration, rhizosphere chemistry, and mineral relations independently of free water at the root surface. Second, we imposed waterlogging in M82 and in two M82 introgression lines, IL11-4 and IL8-1. These lines were selected because previous high-throughput physiological phenotyping identified contrasting whole-plant transpiration and drought-response behavior relative to the recurrent parent M82 (Gosa et al., 2026); they were not preselected for waterlogging tolerance or adventitious-root traits. The study was therefore designed as a physiological comparison between N_2-induced hypoxia and waterlogging, not as a complete factorial separation of all hypoxic, hydraulic, and developmental components of flooding. We hypothesized that (H1) N_2-induced hypoxia reduces whole-plant transpiration and alters rhizosphere chemistry and plant mineral relations, consistent with impaired root function under low oxygen availability, and that (H2) under waterlogging, adventitious-root emergence is associated with a measurable but partial recovery of whole-plant transpiration, whereas N_2-induced hypoxia without water excess does not generate a comparable visible surface-root response under the conditions tested.

2. Results

The experimental framework comprised two N_2-induced hypoxia experiments under non-flooded conditions and one waterlogging experiment (Figs. 1 and 2; Table 1). Experiment 2 is presented in the main figures as the primary N_2-induced hypoxia experiment, and Experiment 1 is presented in the Supplementary Information as a supporting experiment. Because Exp. 1 and Exp. 2 differed in control aeration treatment and in the datasets collected, Exp. 1 was used to evaluate whether the main oxygen, pH, redox, and transpiration trends were reproducible, rather than as a strict replicate of Exp. 2. Exp. 3 extended the analysis to genotype-dependent waterlogging responses but did not include direct measurement of soil O_2.

2.1. N_2-induced hypoxia under non-flooded conditions

Effects of N_2-induced hypoxia on transpiration dynamics, soil pH, and redox potential.

Before N_2 injection in Exp. 2, depth-averaged soil O_2 concentrations were approximately 18%–19% in both treatments. Following the onset of N_2 injection (Fig. 3, red dashed line), soil O_2 concentration in the N_2-induced hypoxia treatment declined rapidly, reaching approximately 1.7% within 1.5 h and stabilizing at 0.09%–0.7%, whereas air-flushed controls remained near 18%–19% (Fig. 3B; Supplementary Fig. S3B). Despite this rapid O_2 depletion, midday whole-plant transpiration did not differ significantly between treatments during the first approximately 20 h. A significant reduction in transpiration under N_2-induced hypoxia developed only after sustained exposure, resulting in a mean decrease of approximately 21%–22% during days 5–10 of treatment in Exp. 2 and days 2–6 in Exp. 1 (Fig. 3A; Supplementary Fig. S3A). This temporal lag indicates that the transpiration response was not an immediate consequence of O_2 depletion, but reflected downstream physiological adjustment to sustained hypoxia.

O_2 depletion was accompanied by changes in soil chemical conditions. Soil pH increased following N_2 injection. This increase was larger relative to the naturally aerated treatment in Exp. 1 than relative to the air-flushed control in Exp. 2, with mean differences of approximately 0.9 and 0.4 pH units, respectively (Fig. 3C; Supplementary Fig. S3C). In Exp. 1, the treatment difference was established within a few hours, whereas in Exp. 2 it developed more gradually and became apparent after approximately 1.5 d. Redox potential (Eh) shifted toward more reducing conditions under N_2-induced hypoxia. Whereas air-flushed controls showed only a modest decline of approximately 50 mV, Eh in N_2-treated columns decreased within the first 15 h and continued to decline thereafter, with mean values of 445 mV in controls and 327 mV under N_2-induced hypoxia across days 5–10 (Fig. 3D; Supplementary Fig. S3D). These values indicate a relative shift toward more reducing conditions, but they remained high compared with strongly reduced

Fig. 1. Experimental platform used to impose N_2-induced hypoxia under non-flooded conditions while continuously monitoring whole-plant and rhizosphere responses in Exp. 1 and Exp. 2. Tomato plants were grown in PVC soil columns mounted on weighing lysimeters (PlantArray 3.0) positioned above drainage containers. N_2-induced hypoxia or aerated control conditions were imposed by continuous delivery of N_2 or air through an inlet tube inserted into the soil column. Rhizosphere pH and redox potential (Eh) were monitored using electrodes inserted through dedicated side ports, and soil O_2 was measured using an oxygen sensor installed in the column wall. Environmental conditions were recorded by the greenhouse weather station. The system enabled continuous gravimetric, environmental, and rhizosphere monitoring throughout the experiment.

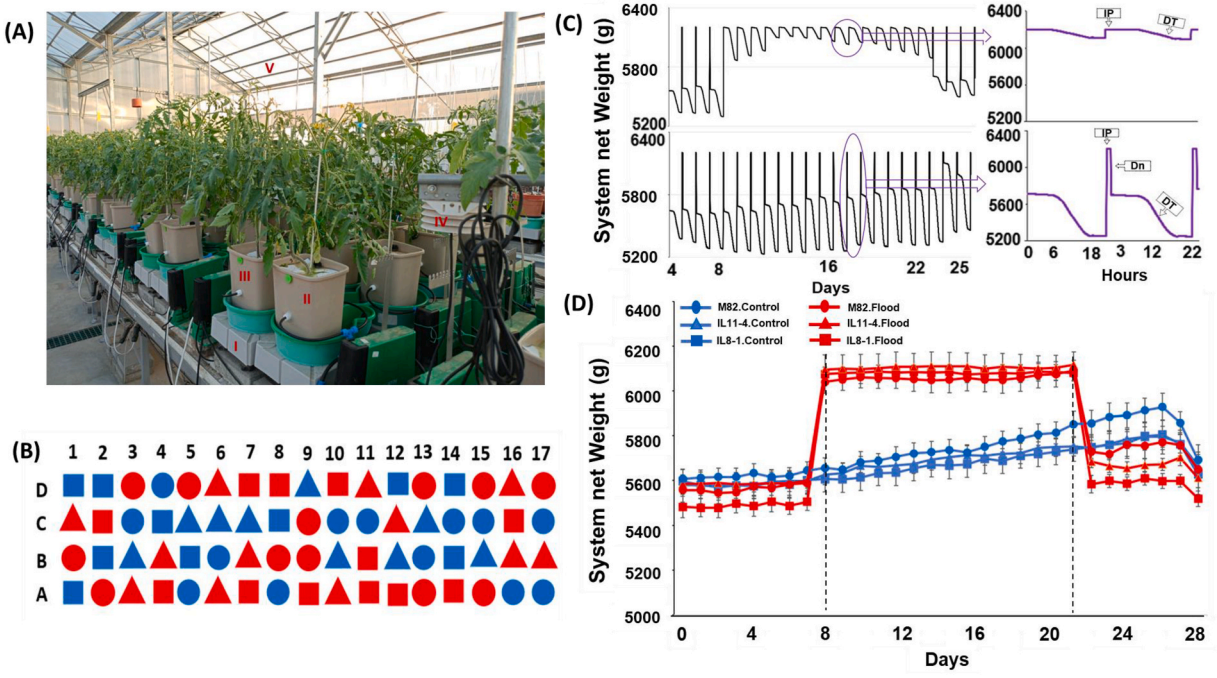

Fig. 2. Waterlogging experimental setup and design in Exp. 3. (A) Photograph of the waterlogging experiment conducted on the PlantArray gravimetric phenotyping platform, showing: (I) lysimeter platform, (II) waterlogged pot, (III) control pot, (IV) greenhouse weather station, and (V) polycarbonate greenhouse. (B) Randomized spatial arrangement of the 68 pots on the platform. Shapes indicate genotypes (M82, circle; IL11-4, triangle; IL8-1, square). Blue symbols denote control plants, and red symbols denote waterlogged plants. (C) Representative system-weight traces illustrating a waterlogged pot (upper trace) and a standard irrigation-drainage pot (lower trace). Changes in system net weight in the waterlogged pot primarily reflect whole-plant transpiration, as drainage is prevented and soil evaporation is minimized by the EVA surface cover. IP, irrigation peak; Dn, drainage; DT, daily transpiration. (D) Daily pre-dawn system weight (plant, soil, and water) measured at 04:00, after drainage and before the onset of daily transpiration. Day indicates days from the start of phenotyping; waterlogging was imposed on day 9 and drainage was restored on day 22. Pre-dawn measurements minimize the effects of diurnal transpiration and short-term irrigation dynamics. Under drained conditions, day-to-day increases in system weight primarily represent plant growth, whereas during waterlogging the system weight also reflects retained water in the flooded root zone. Vertical dashed lines indicate the start and end of the waterlogging period. Lines represent genotype-by-treatment means, with symbols as in (B); waterlogged treatments are shown in red and control treatments in blue. (For interpretation of the references to colour in this figure legend, the reader is referred to the Web version of this article.)

Table 1
Overview of the experimental framework and interpretation limits.

Experiment	Season/ year	Plant material and treatment	Main measurements and interpretation limits
Exp. 1	Spring 2019	M82; N_2-induced hypoxia versus ambient aeration; 8 d treatment followed by 5 d post-treatment	Transpiration, root-zone O_2, pH, redox potential, soil solution. Supporting experiment; not a strict replicate of Exp. 2 because control aeration and measured datasets differed.
Exp. 2	Autumn 2019	M82; N_2-induced hypoxia versus forced air through the same tubing; 7 d treatment	Transpiration, root-zone O_2, pH, redox potential, soil solution, drainage water, leaf and root elemental data. Main N_2-induced hypoxia experiment.
Exp. 3	Autumn 2023	M82, IL11-4, and IL8-1; root-zone waterlogging versus drained control; 14 d waterlogging followed by 7 d recovery	Transpiration, growth, adventitious-root score, stem sections, flowers and fruits. Soil O_2 was not directly measured; adventitious-root score was semi-quantitative.

N_2-induced hypoxia under non-flooded conditions.

waterlogged soils and therefore do not demonstrate the establishment of strongly reducing conditions.

2.2. Elemental concentrations under hypoxia

In Exp. 2, elemental responses to hypoxia were detected mainly in soil solution and drainage water, with more limited, element-specific changes in plant tissues. Under N_2-induced hypoxia, clear treatment effects were detected in the soil solution and drainage, most notably an increase in potassium (K) concentration in drainage water (Fig. 4C). Among microelements, treatment-dependent differences were also observed in both soil solution and drainage, although these responses were element specific and less consistent than those of the macroelements (Fig. 4B–D). In the youngest mature leaf, concentrations of S, Na, K, Ca, and P differed between treatments and were generally higher in ventilated controls, with the exception of Na, indicating treatment-dependent differences in leaf mineral status rather than a uniform inhibition of mineral uptake (Fig. 4E). Magnesium concentration did not differ between treatments (Fig. 4E). In roots, only K showed a significant treatment effect and was higher under oxygen deficiency (Fig. 4G), suggesting altered K retention, redistribution, or root-to-shoot transport under hypoxic conditions. Exp. 1 provided partial support for a soil-solution response to oxygen depletion but was not treated as a direct replicate because the control treatment and measured datasets differed. Before treatment initiation, soil-solution elemental concentrations were similar between treatments (Supplementary Fig. S4A and C). Following hypoxia, K and Mg increased in oxygen-deficient pots, whereas Mn decreased relative to controls, while most other elements showed minor or no changes (Supplementary Fig. S4B and D).

Neither hypoxia experiment induced visible adventitious-root formation under the conditions tested. Because the N_2-induced hypoxia experiments were conducted only in M82 and for shorter periods than the waterlogging experiment, this observation was used as a conservative comparison rather than as evidence that oxygen deficiency cannot contribute to adventitious-root induction. We therefore next compared N_2-induced hypoxia with waterlogging, in which reduced gas diffusion occurs together with free water at the root-zone surface.

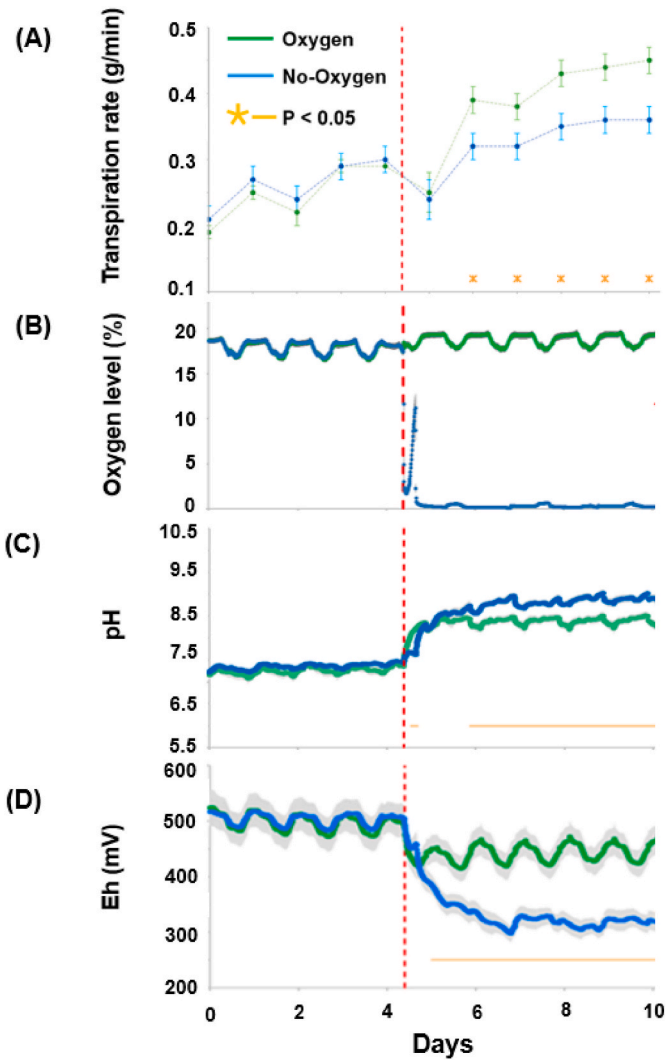

Fig. 3. Overview of key experimental parameters in Exp. 2. Continuous time-series measurements of (A) midday whole-plant transpiration rate, (B) soil O_2 concentration measured at 12.5 and 27.5 cm depths and presented as depth-averaged values, (C) soil pH, and (D) redox potential (Eh). Before treatment, soil O_2 was approximately 18%–19% in both groups. The red dashed line marks the onset of N_2 injection. Data are means ± SE. Yellow markers or horizontal bars indicate time points or intervals with significant differences between the air-flushed control and N_2-induced hypoxia treatments based on Student's t-tests at each time point ($P < 0.05$). Sample sizes were $n = 5$ for the air-flushed control and $n = 4$ for N_2-induced hypoxia in (A), $n = 9$ and $n = 10$, respectively, in (B), $n = 8$ per treatment in (C), and $n = 10$ per treatment in (D). (For interpretation of the references to colour in this figure legend, the reader is referred to the Web version of this article.)

2.3. Waterlogging experiment

Adventitious-root formation and transpiration changes around drainage.

Plants were maintained under standard irrigation-drainage cycles for 8 d, after which waterlogging was imposed by flooding the root zone on day 9. In all genotypes, midday whole-plant transpiration declined rapidly following waterlogging, reaching minimum values on days 13–14, with mean reductions of approximately 16% in M82, 44% in IL11-4, and 55% in IL8-1 relative to their respective controls (Fig. 5A–C). After several days of continuous waterlogging,

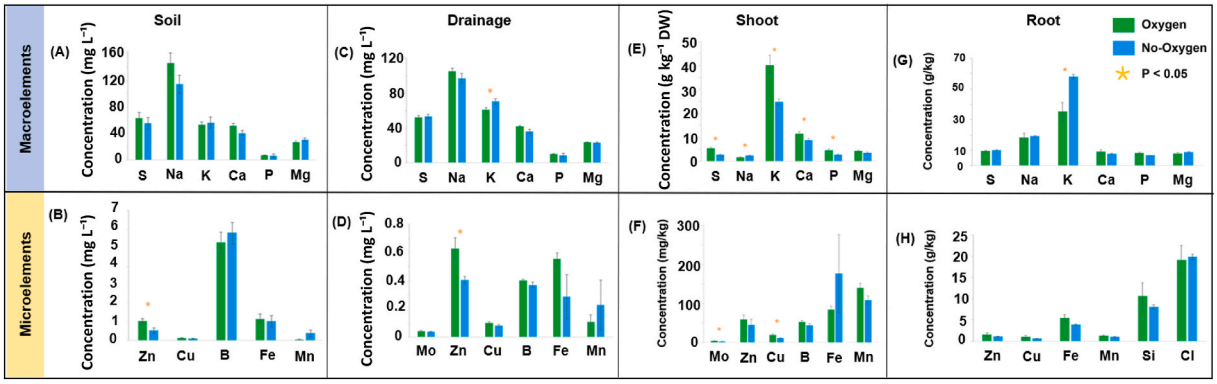

Fig. 4. Elemental concentrations in soil solution, drainage water, and plant tissues under N_2-induced hypoxia in Exp. 2. (A,B) Soil-solution elemental concentrations; (C,D) drainage-water elemental concentrations; (E,F) elemental concentrations in the youngest mature leaf; and (G,H) root elemental abundance determined by SEM-EDS and treated as relative abundance rather than as directly comparable to leaf ICP-AES concentrations. Panels A, C, E, and G show macroelements; panels B, D, F, and H show microelements. Soil-solution and drainage-water concentrations are expressed on a volume basis (mg L^{-1}), and leaf concentrations are expressed on a dry-weight basis. Data are means ± SE. Yellow markers indicate statistically significant differences between treatments for the same element based on Student's t-tests ($P < 0.05$). (For interpretation of the references to colour in this figure legend, the reader is referred to the Web version of this article.)

transpiration showed a transient partial recovery during days 14–22, the period in which adventitious roots were visible at the soil–air interface (Fig. 5A–C,E,G). Adventitious-root formation was strongly genotype dependent: control plants showed few or no adventitious roots, whereas waterlogged plants exhibited significantly higher adventitious-root scores, highest in IL8-1, intermediate in IL11-4, and lowest in M82 (Fig. 5H).

Across individual waterlogged plants, adventitious-root score was negatively correlated with the reduction in transpiration following flooding (Pearson $r = -0.65$; Fig. 5I), such that plants exhibiting stronger adventitious-root development also showed larger absolute reductions in transpiration. Because adventitious roots were scored on a semi-quantitative visual scale, rather than by direct measurements of adventitious-root biomass, volume, area, or hydraulic conductance, this relationship was interpreted as associative rather than causal evidence. The cross-sectional relationship indicates that adventitious-root induction was stronger in plants experiencing greater waterlogging stress. This does not exclude an adaptive function: the time-resolved pattern showed partial transpiration recovery while adventitious roots were visible at the soil–air interface. Thus, adventitious-root abundance may reflect the severity of the inducing stress, whereas the temporal coincidence with partial transpiration recovery is consistent with a possible beneficial contribution. Similar patterns were observed in daily transpiration dynamics (Supplementary Fig. S5).

Genotype-wide treatment effects are shown in Figs. 5 and 6 and were used as the primary basis for comparing waterlogging sensitivity. In addition, we performed a restricted responder-only calculation to describe the whole-plant transpiration change around restoration of drainage in plants in which waterlogging measurably impaired transpiration. The number of responding plants was itself genotype dependent: all waterlogged IL8-1 plants exhibited reduced transpiration, all but one IL11-4 plant showed a reduction, whereas only three M82 plants displayed a clear decrease. Within this responding-plant subset, reductions in daily transpiration relative to genotype-matched controls on days 13–14 amounted to 423.36 ± 3.82 g in M82, 324.22 ± 36.16 g in IL11-4, and 361.60 ± 21.57 g in IL8-1 (insets in Fig. 5A–C). This subset analysis asks a narrower question than the genotype-wide analysis and should not be interpreted as a genotype-wide mean response. On day 22, drainage was restored and plants returned to irrigation-drainage cycles. During days 14–22, mean daily transpiration losses relative to controls decreased to 196.25 ± 43.42 g in M82, 201.53 ± 21.91 g in IL11-4, and 246.65 ± 17.38 g in IL8-1. On the first day after drainage was restored, mean losses increased to 255.57 ± 40.03 g in M82, 259.36 ± 27.51 g in IL11-4, and 314.85 ± 13.73 g in IL8-1. The day 22-to-23 increase was 59.32 g in M82, 57.83 g in IL11-4, and 68.2 g in IL8-1, corresponding to approximately 15%–20% of the initial transpiration loss. This post-drainage difference coincided with loss of surface-water contact by adventitious roots, but drainage simultaneously altered root-zone aeration, water availability, and the conditions experienced by the primary root system. Thus, the post-drainage increase, equivalent to approximately 15%–20% of the initial transpiration loss, is consistent with a limited contribution of surface-associated adventitious roots to whole-plant transpiration, but cannot be attributed exclusively to their function.

Cumulative transpiration and shoot dry weight were both reduced by nearly half in waterlogged IL8-1 and IL11-4 plants relative to their drained controls, whereas M82 showed no significant treatment effect for either trait (Fig. 6A and B). Waterlogging reduced shoot water-use efficiency (WUE), calculated here as shoot dry weight per unit cumulative transpiration, in all three genotypes relative to their controls, with IL8-1 showing the lowest values (Fig. 6C). Shoot length was significantly reduced only in IL8-1, with no significant effect detected in IL11-4 or M82 (Fig. 6D). Root length decreased in IL8-1 and IL11-4 relative to their controls, whereas M82 showed no significant change (Fig. 6E). The root:shoot ratio increased in IL8-1 and IL11-4 relative to their controls, but not in M82 (Fig. 6F). Visual assessment at harvest supported these genotype-dependent morphological responses to waterlogging (Fig. 6G). Under waterlogging, IL8-1 and IL11-4 appeared smaller and showed more leaf wilting than their drained controls, whereas M82 appeared less affected. Root systems of waterlogged IL8-1 and IL11-4 plants also showed browning and lower apparent root mass, whereas M82 roots appeared less affected.

To determine whether the transpiration and growth responses were accompanied by visible changes in plant structure, we examined stem anatomy at harvest. Stem cross-sections taken just above the adventitious-root zone, corresponding to the region shown in Fig. 5D and E, were inspected qualitatively. In the representative waterlogged IL11-4 and IL8-1 sections, the xylem region appeared less uniformly organized and less clearly delineated than in the corresponding controls, whereas the difference was less apparent in M82 (Fig. 7). These observations were not quantified and were not used as independent statistical evidence for hydraulic impairment. Flower and fruit production were also quantified at harvest (Supplementary Fig. S6). Waterlogging tended to reduce fruit number in IL8-1 and IL11-4, whereas M82 maintained higher flower number under waterlogging; these reproductive data were used as supporting observations rather than as central evidence.

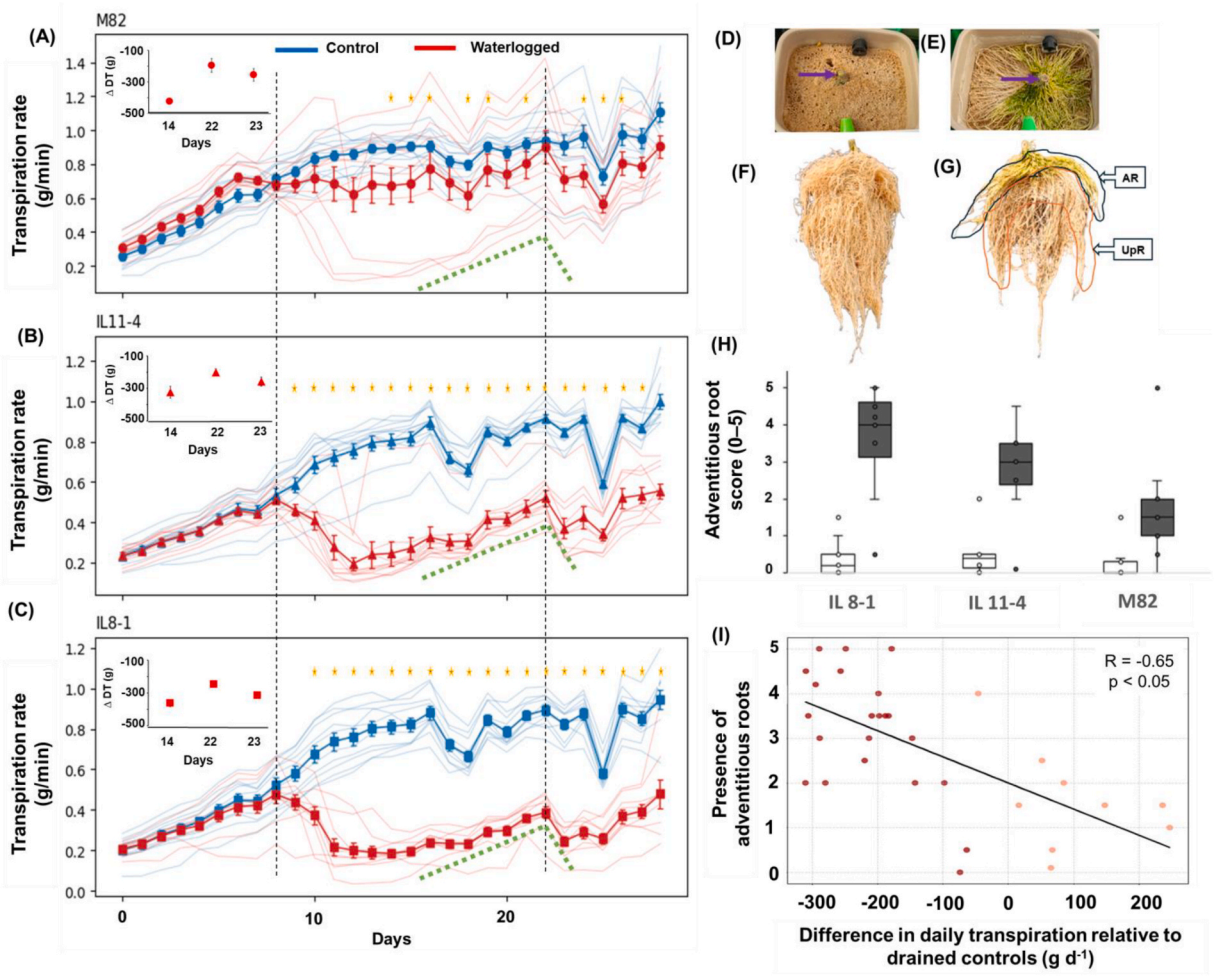

Fig. 5. Whole-plant transpiration dynamics and adventitious-root formation under waterlogging. (A–C) Midday whole-plant transpiration rates during waterlogging in M82 (A), IL11-4 (B), and IL8-1 (C). Bold lines represent means ± SE, and thin lines represent individual plants. Blue lines indicate drained controls, and red lines indicate waterlogged plants. Vertical dashed lines indicate the onset and termination of waterlogging. Yellow stars denote significant differences between treatments at the corresponding time points (Student's t-test, $P < 0.05$). Dashed green lines are visual guides indicating the period during which adventitious roots were visible at the soil–air interface and transpiration partially recovered; they are not fitted models. Insets show the difference in daily transpiration rate relative to the control (ΔDT; g day^{-1}) over the indicated time windows. The day 22-to-23 change is consistent with a contribution of surface-associated adventitious roots to whole-plant water uptake. However, because restoration of drainage simultaneously altered root-zone aeration, water availability, and primary-root conditions, this response cannot be attributed exclusively to adventitious-root function. (D) Representative surface view of a control pot showing no visible adventitious roots. (E) Representative surface view of a waterlogged pot showing adventitious roots emerging at the soil surface. (F) Corresponding whole-root system of the same plant shown in (D), imaged at harvest. (G) Representative whole-root system of a waterlogged plant at harvest, with an annotated schematic highlighting visible adventitious roots (AR) and upper roots (UpR). (H) Adventitious-root scores at harvest (0–5 scale). Open boxes represent controls, and filled boxes represent waterlogged plants. (I) Relationship between the difference in daily transpiration rate relative to drained controls and adventitious-root score under waterlogging. Each point represents an individual waterlogged plant; dark red points: IL11-4 and IL8-1, and light orange points: M82; the line indicates linear regression (Pearson $r = -0.65$, $P < 0.05$). Sample sizes: M82, $n = 11$ per treatment; IL11-4, $n = 12$ controls and $n = 10$ waterlogged plants; IL8-1, $n = 11$ controls and $n = 10$ waterlogged plants. (For interpretation of the references to colour in this figure legend, the reader is referred to the Web version of this article.)

3. Discussion

Our results indicate that the whole-plant response of tomato to waterlogging cannot be inferred from N_2-induced hypoxia alone. Although N_2-induced hypoxia rapidly depleted soil O_2 and altered rhizosphere chemistry, its effect on transpiration developed gradually and did not induce visible adventitious roots under the conditions tested (Fig. 3; Supplementary Fig. S3). In contrast, waterlogging caused a rapid, genotype-dependent decline in transpiration, adventitious-root formation at the soil–air interface, and a transient partial recovery of whole-plant transpiration (Figs. 5 and 6; Supplementary Fig. S5). These findings support a conservative two-layer interpretation: root-zone O_2 limitation constrains whole-plant water and mineral fluxes, whereas the physical and hydraulic configuration of waterlogging adds developmental and functional responses, including surface-root formation and partial transpiration recovery, that were not reproduced by N_2-induced hypoxia. Because oxygen availability was not directly measured during waterlogging and N_2-induced hypoxia was tested only in M82, we do not conclude that adventitious-root formation is independent of hypoxia. Rather, the data show that N_2-induced hypoxia did not reproduce the complete waterlogging response under the conditions tested.

N_2-induced hypoxia imposed a clear and reproducible root-zone oxygen limitation, but the whole-plant transpiration response developed only after sustained exposure. Across the two N_2-induced hypoxia experiments, displacement of soil O_2 by N_2 increased pH and decreased redox potential (Fig. 3C and D; Supplementary Fig. S3C and D), together with shifts in mineral composition in leaves and roots (Fig. 4E–H). The mean Eh of 327 mV under N_2-induced hypoxia was lower than the 445 mV control value but remained relatively high compared with strongly reduced waterlogged soils. Accordingly, the data support a shift

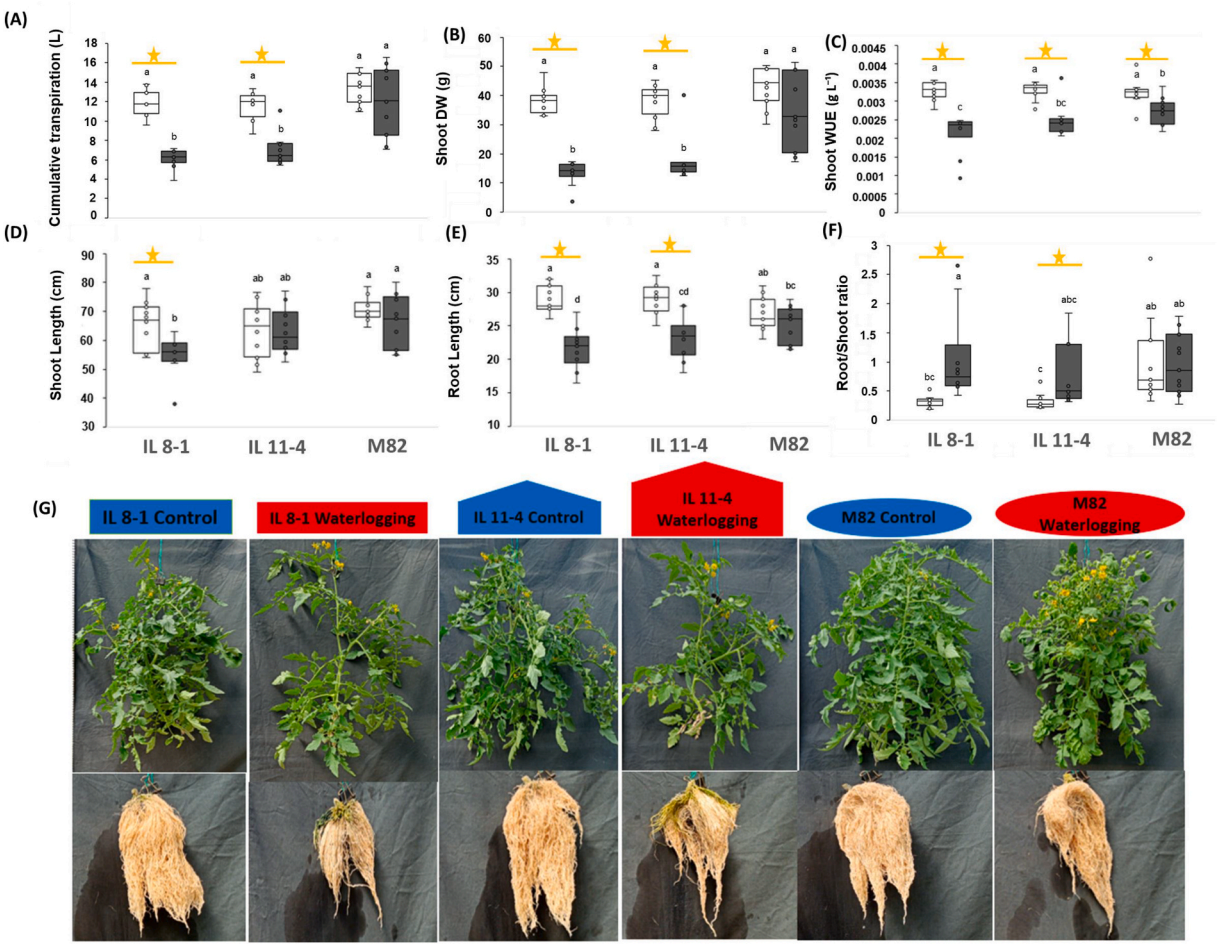

Fig. 6. Effects of waterlogging on transpiration, biomass, water-use efficiency, and plant morphology. (A) Cumulative transpiration. (B) Shoot dry weight at harvest. (C) Shoot water-use efficiency (WUE, g L^{-1}), calculated as shoot dry weight divided by cumulative transpiration. (D) Shoot length. (E) Root length. (F) Root:shoot ratio, calculated using dry biomass. (G) Representative shoots and corresponding root systems of IL8-1, IL11-4, and M82 plants grown under control and waterlogging conditions at harvest; images are shown for visual comparison only and were not used for quantitative size estimation. Data are presented as boxplots. Open boxes represent control plants, and filled boxes represent waterlogged plants. Sample sizes: M82, n = 11 per treatment; IL11-4, n = 12 controls and n = 10 waterlogged plants; IL8-1, n = 11 controls and n = 10 waterlogged plants. Different letters indicate significant differences among genotype-by-treatment groups (one-way ANOVA followed by Tukey's HSD, $P < 0.05$). Yellow lines with stars indicate within-genotype differences between control and waterlogging treatments (Student's t-test, $P < 0.05$). (For interpretation of the references to colour in this figure legend, the reader is referred to the Web version of this article.)

toward more reducing conditions, but not the establishment of strongly reduced conditions or the occurrence of specific reductive processes such as Mn, Fe, or sulfate reduction. The physiological responses are nevertheless consistent with previous studies showing that root-zone hypoxia constrains mitochondrial respiration and cellular ATP production, thereby limiting metabolically demanding processes such as ion uptake and long-distance transport (Wagner et al., 2018; Jethva et al., 2022). The higher K signal in hypoxic roots, together with lower leaf K under the same treatment, suggests altered retention or redistribution of K rather than complete inhibition of K acquisition. Thus, impaired mineral relations should be interpreted as a disruption of whole-plant nutrient transport and allocation, not as absence of root K accumulation.

Mechanistically, these responses are consistent with the expectation that hypoxia-driven ATP limitation reduces plasma-membrane H^+-ATPase activity, thereby depolarizing the membrane potential and weakening the proton-motive force. Such effects would be expected to constrain voltage-dependent transport pathways, including inward-rectifying K^+ channels (Moshelion and Moran, 2000), while a reduced ΔpH would diminish the driving force for H^+-coupled secondary active transport processes (Morsomme and Boutry, 2000). In parallel, the increase in soil pH during N_2-driven gas displacement may also reflect partial removal of dissolved CO_2 from the soil solution, superimposed on the metabolic effects of inhibited root respiration. Because dissolved CO_2 contributes to carbonic acid formation in soil solution, CO_2 stripping by continuous gas flow could contribute to higher pH, consistent with the known sensitivity of flooded and hypoxic soils to gas exchange and redox chemistry (Pezeshki and DeLaune, 2012).

Importantly, the reduction in whole-plant transpiration following O_2 depletion developed progressively over several days (Fig. 3A; Supplementary Fig. S3A), rather than as an abrupt response. This temporal lag argues against immediate hydraulic failure as the primary response to hypoxia and instead supports a gradual decline in root function driven by metabolic impairment. In this framework, reduced respiration under low O_2 would be expected to weaken the energetic and electrochemical basis for solute uptake and allocation, thereby reducing the osmotic component of water uptake. Additional energy-dependent constraints, including possible effects on aquaporin function, may further aggravate this decline (Tournaire-Roux et al., 2003; Boursiac et al., 2008). Thus, the hypoxia-associated reduction in transpiration is better interpreted here as a downstream consequence of metabolic limitation rather than as an immediate hydraulic collapse.

Under waterlogging, whole-plant transpiration in M82 was also reduced, but both the timing of this reduction and the associated developmental responses differed from those observed under N_2-

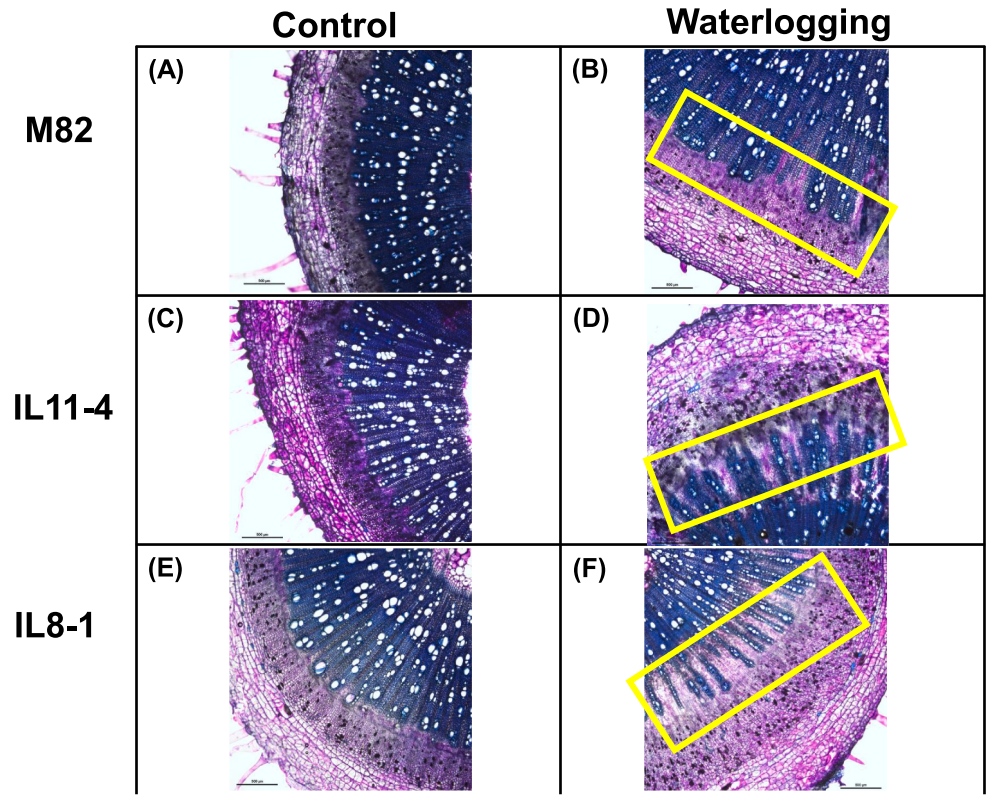

Fig. 7. Toluidine blue-stained tomato stem cross-sections at harvest. (A,B) M82; (C,D) IL11-4; (E,F) IL8-1. Left panels show control plants, and right panels show waterlogged plants. Sections were collected just above the adventitious-root zone. In the representative waterlogged IL11-4 and IL8-1 sections, the xylem region appeared less uniformly organized and less clearly delineated than in the corresponding controls; this difference was less apparent in M82. Yellow boxes identify the regions used for qualitative visual comparison. Xylem area was not quantified, and no statistical anatomical comparison was performed. Scale bars = 500 μm. (For interpretation of the references to colour in this figure legend, the reader is referred to the Web version of this article.)

induced hypoxia. Following the onset of waterlogging, transpiration declined rapidly and reached a minimum within approximately 4–5 d, with a mean reduction of about 16% relative to drained controls (Fig. 5A; Supplementary Fig. S5A). In contrast, N_2-induced hypoxia caused a somewhat larger decline in transpiration in M82, but this response developed more gradually (Fig. 3A; Supplementary Fig. S3A). This difference suggests that waterlogging and N_2-induced hypoxia imposed distinct constraints on root function. N_2 injection likely reduced oxygen availability more uniformly throughout the root zone, whereas under waterlogging oxygen availability may have been more heterogeneous along the soil profile. However, oxygen availability along the waterlogged soil profile was not directly measured, and a uniformly hypoxic root-zone profile should therefore not be assumed. Root acclimation under waterlogging may also involve aerenchyma formation or other anatomical changes that improve internal aeration, responses commonly associated with flooding tolerance (Colmer and Voesenek, 2009; Voesenek and Bailey-Serres, 2015). Because aerenchyma was not quantified here, this remains a plausible mechanism linking waterlogging, root restructuring, and maintenance of water uptake that should be tested directly.

Notably, only a subset of waterlogged M82 plants displayed a pronounced transpiration decline, and these individuals were also characterized by stronger adventitious-root formation (Fig. 5A and H). Across individuals, greater adventitious-root development was associated with a larger transpiration reduction (Fig. 5I). This association indicates that the developmental response was induced most strongly in plants experiencing greater stress, but it should not be interpreted as evidence that adventitious roots were detrimental. Adaptive structures are often induced in proportion to stress severity and may subsequently mitigate, without eliminating, the physiological cost of that stress. The temporal coincidence between adventitious-root visibility and partial transpiration recovery is therefore consistent with a possible beneficial role, whereas the cross-sectional correlation identifies the severity of the inducing stress. This pattern was modest in M82 but much more pronounced in the introgression lines, in which waterlogging caused substantially larger transpiration reductions, approximately 44% in IL11-4 and 55% in IL8-1 relative to controls (Fig. 5A–C; Supplementary Fig. S5A–C). Thus, the genotypes differed markedly in their ability to maintain whole-plant water flux under waterlogging. M82 exhibited relatively small transpiration reductions, low adventitious-root scores (Fig. 5H), and cumulative transpiration comparable to drained controls (Fig. 6A), while maintaining shoot biomass and showing comparatively limited reproductive effects in the supporting observations (Fig. 6B; Supplementary Fig. S6). In contrast, IL11-4 and IL8-1 showed pronounced and sustained transpiration declines, extensive adventitious-root proliferation, reduced shoot growth, lower shoot water-use efficiency, and reduced primary-root development (Fig. 5H,I, 6B–G, and S5B,C). These differences may reflect genotype-dependent variation in ethylene sensitivity, adventitious-root competence, root-zone aeration, or hydraulic vulnerability, all of which should be tested directly before assigning a specific mechanism.

Several, not mutually exclusive, explanations may account for the absence of adventitious-root formation in the N_2-induced hypoxia experiments. First, these experiments were conducted only in M82, a genotype that also exhibited relatively limited adventitious-root formation under waterlogging compared with IL11-4 and especially IL8-1 (Fig. 5H). Second, the duration of the N_2-induced hypoxia treatment was shorter than that of the waterlogging experiment and may have been insufficient to allow full development of this response. Third, oxygen depletion during N_2-induced hypoxia was imposed rapidly,

whereas during waterlogging the decline in rhizosphere O_2 may have developed more gradually. Adventitious-root induction may therefore depend not only on the severity of oxygen limitation, but also on genotype, exposure duration, ethylene-related signaling, and the temporal dynamics of O_2 decline. Thus, under the conditions used here, N_2-induced hypoxia did not reproduce adventitious-root formation, but these experiments do not exclude a role for slower, longer, or genotype-specific hypoxic exposure in triggering this developmental response. Testing N_2-induced hypoxia in IL11-4 and IL8-1 would be a direct next step.

Stem cross-sections taken above the adventitious-root zone provided only qualitative, exploratory observations of the xylem region under waterlogging (Fig. 7). In the representative waterlogged IL11-4 and IL8-1 sections, this region appeared less uniformly organized and less clearly delineated than in controls, but xylem area was not quantified and the images were not used as independent evidence for reduced hydraulic capacity. The transient partial recovery of transpiration during days 14–22 coincided with adventitious-root emergence, and transpiration loss increased again after drainage (Fig. 5A–C; Supplementary Fig. S5A–C, green dashed guides). The day 22-to-23 difference corresponded to approximately 15%–20% of the initial daily transpiration loss. However, restoring drainage simultaneously removed free surface water, increased gas exchange with the root zone, changed water availability, and may have altered the condition and function of the primary root system. Waterlogging may also have caused primary-root mortality while newly formed adventitious roots, which can be more porous, partially replaced root function. Consequently, the post-drainage response provides indirect, non-exclusive evidence consistent with a limited contribution of surface-associated adventitious roots to whole-plant transpiration. It does not isolate or precisely quantify that contribution, because drainage simultaneously changed several root-zone conditions.

Together, these results indicate that adventitious rooting had two distinguishable associations under waterlogging. Greater root development occurred in the more strongly affected plants, identifying the severity of the inducing stress, whereas root visibility also coincided temporally with partial transpiration recovery, consistent with a possible adaptive role in maintaining water transport. The present design does not separate these two relationships causally. Adventitious-root formation was not reproduced by the N_2-induced hypoxia treatment used here. This difference may reflect exposure duration, genotype, the temporal pattern of O_2 decline, or additional hydraulic, chemical, or mechanical cues associated with water excess.

3.1. Limitations and interpretation

Several limitations define the scope of the present interpretation. First, soil O_2 was directly measured in the N_2-induced hypoxia experiments but not during waterlogging; therefore, the comparison does not define the exact oxygen environment experienced by roots in Exp. 3. Second, N_2-induced hypoxia was tested only in M82, whereas genotype-dependent responses were assessed under waterlogging. Third, adventitious-root development was evaluated using a semi-quantitative visual score rather than direct measurements of adventitious-root biomass, area, volume, or hydraulic conductance. Fourth, the anatomical observations in Fig. 7 are qualitative and should not be used as quantitative evidence for changes in xylem capacity. Fifth, restoration of drainage simultaneously altered surface-water access, root-zone aeration, water availability, and primary-root conditions; therefore, the post-drainage transpiration change cannot be assigned specifically to adventitious-root function. These limitations constrain precise causal attribution but do not alter the temporal association between adventitious-root emergence, partial transpiration recovery, and renewed decline after drainage. They also preserve the central physiological contrast: N_2-induced hypoxia under non-flooded conditions did not reproduce the full waterlogging response, and adventitious-root emergence was associated with both greater stress severity and transient partial recovery of transpiration.

4. Conclusions

In tomato, N_2-induced hypoxia and waterlogging shared root-zone oxygen limitation but produced distinct whole-plant trajectories. N_2-induced hypoxia rapidly altered root-zone O_2, pH, redox potential, and mineral relations, whereas transpiration declined only after sustained exposure. Waterlogging caused a faster, genotype-dependent decline and induced adventitious roots whose emergence coincided with transient recovery of transpiration. Stronger rooting was associated with greater stress, and the post-drainage response was consistent with a limited, non-exclusive contribution of surface-associated adventitious roots to whole-plant transpiration. Adventitious roots are therefore best interpreted here as a stress-induced acclimation response that may support partial recovery but does not restore whole-plant transpiration. These time-resolved measurements provide a physiological framework for distinguishing responses to rapid oxygen depletion from waterlogging-specific acclimation.

5. Materials and methods

5.1. Plant material and growth conditions

Tomato plants (*Solanum lycopersicum*) from three lines were used: cv. M82 and the two introgression lines IL11-4 and IL8-1 (Eshed and Zamir, 1995). These lines were previously characterized as differing in whole-plant transpiration and drought-response behavior and were selected to test whether genotypes with contrasting transpiration phenotypes also differ in waterlogging response (Gosa et al., 2026). The irrigation solution composition is provided in Supplementary Table S1.

All experiments were conducted in the iCORE functional-phenotyping greenhouse at the Faculty of Agriculture, Food and Environment, Rehovot, Israel, during three experimental periods: Exp. 1 in spring 2019, Exp. 2 in autumn 2019, and Exp. 3 in autumn 2023. The polycarbonate greenhouse allowed partial environmental control while maintaining semi-natural fluctuations in light and vapor pressure deficit (VPD) (Supplementary Fig. S1). Photosynthetic photon flux density (PPFD), air temperature, relative humidity, and VPD were continuously recorded by an in-greenhouse weather station.

Continuous whole-plant transpiration was measured using the high-throughput gravimetric functional-phenotyping system PlantArray 3.0 (Plant-DiTech, Israel). Plant weight was recorded at 3-min intervals using load cells, and transpiration was calculated from changes in pot weight over time. Data were processed using SPAC Analytics software (Plant-DiTech). Detailed descriptions of system operation and validation are provided in Halperin et al. (2017), Yaaran et al. (2019), and Dalal et al. (2020).

To isolate the effects of root-zone oxygen deficiency independently of soil water excess, we used a controlled soil-column system in which oxygen was displaced from soil pore space by N_2 gas, thereby imposing hypoxic conditions while maintaining soil structure and water-holding capacity under regular irrigation at near-field-capacity conditions (Fig. 1). In experiment 1 (Exp. 1), the N_2 treatment was compared with natural oxygen supply from the soil surface. In experiment 2 (Exp. 2), the N_2 treatment was compared with atmospheric air supplied through the same tubing system at a similar flow rate. Each experiment included 10 individual plant/soil-column units ($n = 10$), which should be interpreted as within-experiment plant replicates rather than independent repeat experiments. The columns were constructed from rigid PVC cylinders (internal diameter, 10.6 cm; height, 43 cm). Prior to treatment initiation, plants were acclimated to the system and baseline physiological measurements were established.

Hypoxic conditions were generated by continuously supplying high-purity N_2 gas (99.999%) through flexible silicone tubing inserted into

each column at depths of 22 and 29 cm below the soil surface. In Exp. 2, aerated control columns received atmospheric air through an identical tubing configuration. Gas was dispersed within the soil using an air stone positioned at the end of the tube. To prevent soil desiccation during continuous gas flow, the gas was humidified by bubbling through water in a sealed 1.5-L bottle before entering the columns (Supplementary Fig. S2).

Control conditions differed between experiments. In Exp. 1, control plants were maintained under ambient soil aeration without gas injection. In Exp. 2, to control for possible effects of continuous gas flow itself, including CO_2 stripping, atmospheric air was supplied through the same tubing system using a small aquarium pump at low flow. This control air was also humidified before entering the soil (Supplementary Fig. S2). In Exp. 1, N_2 flow was applied continuously for 8 days, followed by a 5 days post-treatment period without gas injection. In Exp. 2, N_2 or air flow was applied continuously for 7 days.

To enable repeated monitoring along the soil profile, six access ports were installed at fixed depths: three at 12.5 cm and three at 27.5 cm below the soil surface (diameter, 2 cm). The ports were sealed with cable adapters, allowing insertion of sensors and electrodes without external air infiltration. At each depth, a redox (oxidation-reduction potential, ORP) electrode, a pH electrode, and a soil-solution sampling port were installed. An opposing port (diameter, 3 cm) housed a horizontally mounted oxygen sensor in a sealed plastic holder.

5.2. Oxygen, redox, pH, and soil water content measurements

Two KE-50 oxygen sensors (Figaro Engineering Inc., Japan) were installed in each soil column at depths of 12.5 and 27.5 cm. Each sensor was housed in a perforated plastic tube (20 ± 2 holes, approximately 1 mm in diameter), forming an equilibration chamber that allowed direct exchange with soil pore gas. The housing was kept in direct contact with the surrounding sand matrix to ensure equilibration with the soil atmosphere rather than with a sealed headspace. Sensor insertion points were sealed with silicone adhesive sealant to prevent external air intrusion.

Redox potential was measured using wide-band platinum electrodes with Ag/AgCl reference cells (ELH-031, Van London Phoenix Co., USA), installed at the same depths as the oxygen sensors and sealed with PG16 adapters. Soil pH was measured using $Ag/AgCl^{-}$ based pH electrodes (ELH-067, Van London Phoenix Co., USA), installed and sealed at the same depths as the redox electrodes.

In each column, 5 TE volumetric water-content sensors (Meter Group, USA) were inserted vertically to continuously measure volumetric water content (VWC), temperature, and electrical conductivity (EC) at the two sensor depths. All sensors were connected to the PlantArray controller or to separate dataloggers for continuous data logging.

5.3. Soil solution characterization

Soil solution samples were collected using syringes connected to Rhizon samplers (Rhizosphere Research Products, Wageningen, The Netherlands) installed at the two sensor depths. Soil solution was sampled 2 d before treatment initiation and several hours after treatment termination. Macro- and micronutrient concentrations were quantified by inductively coupled plasma atomic emission spectroscopy (ICP-AES; ARCOS, SPECTRO GmbH, Kleve, Germany) and expressed on a volume basis (mg L^{-1}).

5.4. Harvesting and tissue analysis

At the end of the experiment, drainage water was collected from the base of each pot and analyzed for elemental composition by ICP-AES. Drainage-water elemental concentrations were expressed on a volume basis (mg L^{-1}). The youngest fully expanded leaf was harvested, fresh weight was recorded, and the tissue was dried at 60 °C for 4 d and ground to a fine powder. For elemental analysis, 100 mg of dry tissue was digested in concentrated nitric acid, heated, and then treated with perchloric acid. The digests were diluted and analyzed by ICP-AES.

Roots were thoroughly rinsed to remove sand, immediately frozen in liquid nitrogen, and stored at −80 °C until analysis. Root elemental composition was determined using low-vacuum scanning electron microscopy coupled with energy-dispersive X-ray spectroscopy (SEM-EDS; JEOL IT100). These root SEM-EDS measurements were used as relative elemental abundance data and were not treated as directly comparable to the ICP-AES leaf concentrations.

5.5. Waterlogging experiment

The waterlogging experiment corresponds to Exp. 3. In this experiment, only the root zone was flooded; therefore, the term waterlogging is used rather than flooding. No direct manipulation or measurement of oxygen availability was applied during Exp. 3. Changes in rhizosphere oxygen availability therefore arose solely from waterlogging-induced limitations to gas diffusion and were not assumed to be spatially uniform. Seeds were germinated and grown as described above. One 3-week-old plant was transplanted into each 5-L waterlogging pot (Plant-DiTech “Flood Control Kit” prototype) and placed on the phenotyping platform (Fig. 2A). The experiment included 68 pots arranged in a completely randomized design, with 10–12 individual plant/pot replicates per genotype and treatment (Fig. 2B). Following acclimation under standard irrigation-drainage cycles, waterlogging was imposed on half of the plants by closing the drainage outlet, resulting in flooding of the root zone (Fig. 2C). Waterlogging was maintained for 2 weeks, after which plants were returned to normal irrigation-drainage conditions for a 1-week recovery period prior to harvest (Fig. 2D). Transpiration loss was calculated for each waterlogged plant as $\Delta DT(d) =$ mean daily transpiration (DT) of the genotype-matched drained controls on day d − DT of the waterlogged plant on day d. Initial loss was defined as the mean ΔDT on days 13–14. The period of partial recovery was defined as days 14–22, when adventitious roots were visible at the soil–air interface. The post-drainage transpiration change was calculated as ΔDT(day 23) − ΔDT(day 22), where day 23 represents the first day after drainage was restored, and was also expressed relative to the initial loss as $100 \times$ [ΔDT(day 23) − ΔDT(day 22)]/initial loss. This contrast describes the whole-system change around drainage. It cannot be attributed exclusively to adventitious-root water uptake because restoring drainage simultaneously removed the surface water layer and altered root-zone aeration, water availability, and primary-root conditions. For the responder-only analysis in Fig. 5, the included waterlogged plants comprised all IL8-1 plants exhibiting reduced transpiration, all but one IL11-4 plant showing a reduction, and the three M82 plants displaying a clear decrease during the initial decline window (days 13–14). This responder-only calculation was not used as the sole basis for genotype-wide treatment comparisons.

5.6. Measurement of agro-morphological parameters

Adventitious roots emerging on the sand surface were scored on a 0–5 scale (0, none visible; 5, surface fully covered). Scoring was performed by a single observer using predefined criteria and applied consistently across all treatments. This score is semi-quantitative and reflects visible surface coverage rather than adventitious-root biomass or volume. At harvest, shoot and root length, fresh and dry biomass, and the numbers of flowers and fruits were recorded.

5.7. Stem section preparation and analysis

The aerial stem portion was excised immediately above the adventitious-root zone, when present, and a fresh 10-cm segment was fixed in 70% ethanol. Transverse sections (approximately 100 µm thick) were prepared using a rotary microtome (Leica RM2255; TC-65

disposable blades), stained with 0.1% (w/v) toluidine blue, and imaged under bright-field illumination using an Olympus BX53 microscope equipped with a DP73 camera. The images shown in Fig. 7 are representative qualitative sections; xylem area was not quantified and no statistical anatomical comparison was performed.

5.8. Statistical analysis

Data were processed using SPAC Analytics (Plant-DiTech, Israel) and JMP Pro 18.0 (SAS Institute). In the N_2-induced hypoxia experiments, time-series treatment comparisons for transpiration, soil O_2, pH, and redox potential were performed at each measured time point using Student's t-test. Elemental concentrations in soil solution, drainage water, leaves, and roots were compared between treatments using Student's t-tests for each element. In the waterlogging experiment, genotype-by-treatment harvest traits were analyzed by one-way ANOVA followed by Tukey's HSD, with additional within-genotype Student's t-tests where indicated in the figure legends. Relationships between adventitious-root score and transpiration loss were evaluated using Pearson correlation. Time-series significance markers were used to identify periods of treatment divergence and were interpreted together with the physiological time course, rather than as independent endpoint tests. Significance was assessed at $P < 0.05$. Sample sizes and tests are specified in the corresponding figure legends.

Funding

This project was funded by the Planning and Budgeting Committee of the Council for Higher Education in Israel (VATAT) as part of the program "Israeli Center for Digital Agriculture." Additional support was provided by an individual postdoctoral fellowship from the Azrieli Foundation awarded to H.P., and by the Israel Ministry of Agriculture and Rural Development (Eugene Kandel Knowledge Centers) through the project "Root of the Matter – The root zone knowledge center for leveraging modern agriculture" (Grant No. 391-15). The funding sources had no role in study design, data collection, data analysis, interpretation of the results, manuscript preparation, or the decision to submit the work for publication.

CRediT authorship contribution statement

Hermann Prodjinoto: Investigation, Writing – original draft, Writing – review & editing. **Dor Batat:** Formal analysis. **Ido Nir:** Writing – review & editing. **Dana Menkes:** Conceptualization, Investigation, Writing – original draft. **Moshe Shenker:** Conceptualization, Formal analysis, Investigation, Methodology, Supervision, Writing – original draft. **Menachem Moshelion:** Conceptualization, Data curation, Formal analysis, Methodology, Supervision, Validation, Writing – original draft, Writing – review & editing.

Declaration of competing interest

The authors declare that they have no known competing financial interests or personal relationships that could have appeared to influence the work reported in this paper.

Acknowledgements

H.*P. and* M.M. gratefully acknowledge the funding and support provided by the Azrieli Foundation to H.P. through their International Postdoctoral Fellowship Programme.

Appendix A. Supplementary data

Supplementary data to this article can be found online at https://doi.org/10.1016/j.jplph.2026.154850.

Data availability

The datasets generated and/or analyzed during the current study are available from the corresponding authors upon reasonable request.

References

Boursiac, Y., Boudet, J., Postaire, O., Luu, D., Tournaire-Roux, C., Maurel, C., 2008. Stimulus-induced downregulation of root water transport involves reactive oxygen species-activated cell signalling and plasma membrane intrinsic protein internalization. Plant J. 56, 207–218. https://doi.org/10.1111/j.1365-313X.2008.03594.x.

Calvo-Polanco, M., Señorans, J., Zwiazek, J.J., 2012. Role of adventitious roots in water relations of tamarack (*Larix laricina*) seedlings exposed to flooding. BMC Plant Biol. 12, 99. https://doi.org/10.1186/1471-2229-12-99.

Colmer, T.D., Voesenek, L., 2009. Flooding tolerance: suites of plant traits in variable environments. Funct. Plant Biol. 36, 665–681. https://doi.org/10.1071/FP09144.

Dalal, A., Shenhar, I., Bourstein, R., Mayo, A., Grunwald, Y., Averbuch, N., Attia, Z., Wallach, R., Moshelion, M., 2020. A telemetric, gravimetric platform for real-time physiological phenotyping of plant–environment interactions. JoVE (Journal of Visualized Experiments), e61280. https://doi.org/10.3791/61280.

Eshed, Y., Zamir, D., 1995. An introgression line population of Lycopersicon pennellii in the cultivated tomato enables the identification and fine mapping of yield-associated QTL. Genetics 141, 1147–1162. https://doi.org/10.1093/genetics/141.3.1147.

Gosa, S.C., Gebeyo, B.A., Patil, R., Mencia, R., Moshelion, M., 2026. Stomatal density and aperture dynamics regulate drought response and yield in tomato. Plant Sci. 370, 113170. https://doi.org/10.1016/j.plantsci.2026.113170.

Halperin, O., Gebremedhin, A., Wallach, R., Moshelion, M., 2017. High-throughput physiological phenotyping and screening system for the characterization of plant–environment interactions. Plant J. 89, 839–850. https://doi.org/10.1111/tpj.13425.

Horchani, F., Khayati, H., Raymond, P., Brouquisse, R., Aschi-Smiti, S., 2009. Contrasted effects of prolonged root hypoxia on tomato root and fruit (*Solanum lycopersicum*) metabolism. J. Agron. Crop Sci. 195, 313–318. https://doi.org/10.1111/j.1439-037X.2009.00363.x.

Jackson, W.T., 1956. The relative importance of factors causing injury to shoots of flooded tomato plants. Am. J. Bot. 43, 637–639. https://doi.org/10.2307/2438827.

Jethva, J., Schmidt, R.R., Sauter, M., Selinski, J., 2022. Try or die: dynamics of plant respiration and how to survive low oxygen conditions. Plants 11, 205. https://doi.org/10.3390/plants11020205.

Kęska, K., Szcześniak, M.W., Makałowska, I., Czernicka, M., 2021. Long-term waterlogging as factor contributing to hypoxia stress tolerance enhancement in cucumber: comparative transcriptome analysis of waterlogging sensitive and tolerant accessions. Genes 12, 189. https://doi.org/10.3390/genes12020189.

Kuo, C.G., Chen, B.W., 1980. Physiological responses of tomato cultivars to flooding. J. Am. Soc. Hortic. Sci. 105, 751–755. https://doi.org/10.21273/JASHS.105.5.751.

Leyshon, A.J., Sheard, R.W., 1974. Influence of short-term flooding on the growth and plant nutrient composition of barley. Can. J. Soil Sci. 54, 463–473. https://doi.org/10.4141/cjss74-060.

McNamara, S.T., Mitchell, C.A., 1990. Adaptive stem and adventitious root responses of two tomato genotypes to flooding. Hortscience 25, 100–103. https://doi.org/10.21273/HORTSCI.25.1.100.

Morsomme, P., Boutry, M., 2000. The plant plasma membrane H^+-ATPase: structure, function and regulation. Biochim. Biophys. Acta Biomembr. 1465, 1–16. https://doi.org/10.1016/S0005-2736(00)00128-0.

Moshelion, M., Moran, N., 2000. Potassium-efflux channels in extensor and flexor cells of the motor organ of Samanea saman are not identical. Effects of cytosolic calcium. Plant Physiol. 124, 911–919. https://doi.org/10.1104/pp.124.2.911.

Pan, J., Sharif, R., Xu, X., Chen, X., 2021. Mechanisms of waterlogging tolerance in plants: research progress and prospects. Front. Plant Sci. 11, 627331. https://doi.org/10.3389/fpls.2020.627331.

Pezeshki, S.R., DeLaune, R.D., 2012. Soil oxidation-reduction in wetlands and its impact on plant functioning. Biology 1, 196–221. https://doi.org/10.3390/biology1020196.

Sauter, M., 2013. Root responses to flooding. Curr. Opin. Plant Biol. 16, 282–286. https://doi.org/10.1016/j.pbi.2013.03.013.

Sauter, M., Steffens, B., 2014. Biogenesis of adventitious roots and their involvement in the adaptation to oxygen limitations. In: Van Dongen, J.T., Licausi, F. (Eds.), Low-Oxygen Stress in Plants. Springer, Vienna, Vienna, pp. 299–312. https://doi.org/10.1007/978-3-7091-1254-0_15.

Tournaire-Roux, C., Sutka, M., Javot, H., Gout, E., Gerbeau, P., Luu, D.-T., Bligny, R., Maurel, C., 2003. Cytosolic pH regulates root water transport during anoxic stress through gating of aquaporins. Nature 425, 393–397. https://doi.org/10.1038/nature01853.

Vidoz, M.L., Loreti, E., Mensuali, A., Alpi, A., Perata, P., 2010. Hormonal interplay during adventitious root formation in flooded tomato plants. Plant J. 63, 551–562. https://doi.org/10.1111/j.1365-313X.2010.04262.x.

Voesenek, L.A.C.J., Bailey-Serres, J., 2015. Flood adaptive traits and processes: an overview. New Phytol. 206, 57–73. https://doi.org/10.1111/nph.13209.

Wagner, S., Van Aken, O., Elsässer, M., Schwarzländer, M., 2018. Mitochondrial energy signaling and its role in the low-oxygen stress response of plants. Plant Physiol. 176, 1156–1170. https://doi.org/10.1104/pp.17.01387.

Yaaran, A., Negin, B., Moshelion, M., 2019. Role of guard-cell ABA in determining steady-state stomatal aperture and prompt vapor-pressure-deficit response. Plant Sci. 281, 31–40. https://doi.org/10.1016/j.plantsci.2018.12.027.

Zhang, M., Zhai, G., He, T., Wu, C., 2023. A growing global threat: long-term trends show cropland exposure to flooding on the rise. Sci. Total Environ. 899, 165675. https://doi.org/10.1016/j.scitotenv.2023.165675.

Zhang, Q., Huber, H., Beljaars, S.J.M., Birnbaum, D., de Best, S., de Kroon, H., Visser, E.J. W., 2017. Benefits of flooding-induced aquatic adventitious roots depend on the duration of submergence: linking plant performance to root functioning. Ann. Bot. 120, 171–180. https://doi.org/10.1093/aob/mcx049.